INVITED PAPER

Powering a Ventricular Assist Device (VAD) With the Free-Range Resonant Electrical Energy Delivery (FREE-D) System

This paper discusses wireless delivery of power from a distant source to an implanted cardiac device, and it proposes recharging implanted batteries using magnetically coupled resonators.

By Benjamin H. Waters, *Student Member IEEE*, Alanson P. Sample, *Student Member IEEE*, Pramod Bonde, *Member IEEE*, and Joshua R. Smith, *Member IEEE*

ABSTRACT | Wireless data communication technology has eliminated wired connections for data transfer to portable devices. Wireless power technology offers the possibility of eliminating the remaining wired connection: the power cord. For ventricular assist devices (VADs), wireless power technology will eliminate the complications and infections caused by the percutaneous wired power connection. Integrating wireless power technology into VADs will enable VAD implants to become a more viable option for heart failure patients (of which there are 80 000 in the United States each year) than heart transplants. Previous transcutaneous energy transfer systems (TETS) have attempted to wirelessly power VADs [1]; however, TETS-based technologies are limited in range to a few millimeters, do not tolerate angular misalignment, and suffer from poor efficiency. The free-range resonant electrical delivery (FREE-D) wireless power system aims to use magnetically coupled resonators to efficiently transfer power across a distance to a VAD implanted in the human body, and to provide robustness to geometric changes. Multiple resonator configurations are implemented to improve the range and efficiency of wireless power transmission to both a commercially available axial pump [2] and a VentrAssist centrifugal pump [3]. An adaptive frequency tuning method allows for maximum power transfer efficiency for nearly any angular orientation over a range of separation distances. Additionally, laboratory results show the continuous operation of both pumps using the FREE-D system with a wireless power transfer efficiency upwards of 90%.

KEYWORDS | Magnetically coupled resonators; ventricular assist device (VAD); wireless power

I. INTRODUCTION

Wireless power transfer using inductive coupling is becoming increasingly popular for consumer electronic devices. Commercial applications include wireless charging pads, electronic toothbrushes, induction cookers, and electric car battery chargers. However, none of these applications enable the geometric freedom that the term "wireless power" suggests. Charging pads and electric toothbrushes require that the device be placed very close by or directly on top of the charging pad. This is because the efficiency for inductively coupled wireless power

Manuscript received July 5, 2011; accepted August 10, 2011. Date of publication October 3, 2011; date of current version December 21, 2011.
B. H. Waters, **A. P. Sample**, and **J. R. Smith** are with the Electrical Engineering Department, University of Washington, Seattle, WA 98195-2500 USA (e-mail: bhw2114@uw.edu).
P. Bonde is with the Yale School of Medicine, New Haven, CT 06520 USA.
Digital Object Identifier: 10.1109/JPROC.2011.2165309

transfer systems drops off rapidly as the distance between the transmitter (Tx) and the receiver (Rx) increases.

Range and mobility can be increased with resonant coupling techniques. The free-range resonant electrical delivery (FREE-D) system enables true wireless power transfer by allowing devices to be charged in free space, without direct physical contact between the Tx and the Rx. Within the FREE-D system's working range, power transfer efficiency can be held constant even as Tx–Rx distance and orientation change; beyond the working range, efficiency drops. The working range is dependent on the size of the Tx and Rx resonators: as a rule of thumb, the working range is on the order of the resonator diameter [4].

In this work, we demonstrate that the FREE-D system is able to wirelessly power a ventricular assist device (VAD). First, the benefits of implementing wireless power to the VAD are discussed. A circuit model of the FREE-D resonators is then presented and the system is experimentally tested with two different VADs. This paper also presents a novel range adaptation technique that allows single-frequency operation. Additionally, a method for extending the range of the FREE-D system using relay resonators is presented.

II. THE NEED FOR MAGNETICALLY COUPLED RESONATORS IN MEDICAL APPLICATIONS

A. The Wireless Power Solution

The applications that can currently benefit most from resonantly coupled wireless power transfer systems are those that require dynamic charging, large separation distances between the Tx and the Rx, and do not have highly conductive materials around the resonators that can limit the wireless power transfer range. The VAD fits all of these ideal requirements in that the patient is actively moving and consequently constantly changing the distance and angle between the Tx resonator and the implanted Rx resonator, and the integration of wireless power will hugely benefit the technology in general because the potentially infectious percutaneous driveline will be eliminated.

B. The Medical Problem

Heart failure is a terminal disease with a very poor prognosis and constitutes Medicare's greatest area of spending with annual spending close to $35 billion [5]. The most desirable treatment for heart failure remains a full heart transplant, however, only a limited number (approximately 2000 per year) of patients can benefit from transplants due to donor shortages and high costs. An alternative which has become increasingly popular is mechanical circulatory assistance with ventricular assist devices in which a pump with a central rotor accelerates blood throughout the body [2], [3]. The first generation VADs were approved for use in the United States by the Food and Drug Administration (FDA) in October 1994. The pumps require a percutaneous driveline, meaning a biocompatible cable protrudes from the body to connect the VAD to a power source and the VAD system controller. The system controller communicates with the heart pump to modify pump conditions and simultaneously provide power to the VAD from either a battery for portable use or a central power supply unit (PSU). The typical configuration for a VAD can be seen in Fig. 1. VAD technology has significantly improved in the past 15 years. Initially, VADs were a temporary alternative solution to heart transplants: supporting patients for only a few months. Now, VADs can survive patients for upwards of five years [6], [7]. As a result of the extended lifetime of the VAD, the most common cause for patient readmission to the hospital and patient death is no longer the technical failure of the VAD, but rather the exit site infection (ESI) from the percutaneous driveline. The increasing risk of ESI hampers the patient's quality of life and can lead to repeated hospitalizations for antibiotic treatment, surgical interventions, or even a costly VAD replacement [14].

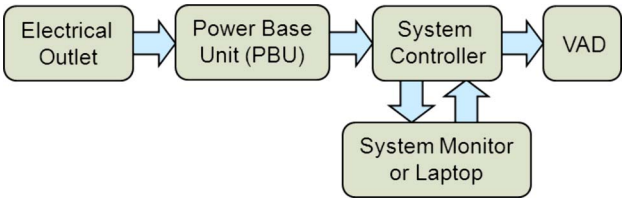

Fig. 1. *Typical configuration for a VAD showing the power base unit (PBU) directly charging the VAD system controller, which is controlled by the system monitor (typically a laptop) to power the VAD and define pump operating conditions. The PBU can be temporarily replaced with a battery for portable use away from an electrical outlet.*

Medical research has demonstrated the relationship between ESI, pump pocket infection—infection in the abdominal pocket where the VADs are implanted—and subsequent sepsis—bacterial growth in the bloodstream [8]–[13]. Seventy percent of VAD patients' first readmission to the hospital is due to ESI [14]. Patients who develop ESI spend more time in the hospital and have ten times as many readmissions as the patients without ESI [15]. The net result of these effects from ESI is the reduced survival and increased cost negating the intended benefit of VAD therapy. Implementing the FREE-D wireless power system to power the VAD pump will eliminate the need for the percutaneous driveline, and consequently eliminate ESI.

C. Limitations With Inductive Charging Using the TETS System

Previous attempts have been made to wirelessly power VADs using transcutaneous energy transfer systems (TETS) [16]–[19]. TETS uses inductive coupling techniques to transfer power between coils on the inner and outer surfaces of the skin. After several decades of

laboratory testing and prototype development, the clinical application of TETS has been possible in only two systems (Arrow LionHeart and AbioCor TAH) [17], [18]. The clinical and laboratory experiments have demonstrated several drawbacks with the current TETS technology. Restrictions on misalignment between the transmitting and receiving coils and the necessity for a close separation distance between the coils limit the practicality of TETS. The system also incurs significant wireless energy loss beyond 10-cm separation. The proximity limitation requires that the receiving coil be implanted just under the skin and the external transmitting coil be secured in a single position on the skin surface with adhesives. For angular misalignments or excessive separation between the coils, the transmitter will attempt to supply more power to account for the reduced efficiency. This effect has proven to cause skin irritability and thermal injury from the increase in coil temperature due to greater power transmission, which can result in burns and lead to infection on the exterior surface of the skin. The TETS technology was first implemented with the Arrow LionHeart VAD in 2001; however, it has since been withdrawn from the market [18].

D. Improvements With Resonant Coupling Using the FREE-D System

The FREE-D system provides wireless power to a VAD using strong resonant coupling technology. FREE-D affords seamless energy supply without compromising mobility or requiring direct contact between the individual and energy source as in TETS. The FREE-D wireless power resonators efficiently transfer power across meter distances to a VAD implanted in the human body [20], [21]. The Tx and Rx resonators are coils of wire that are tuned to resonate at a specific frequency. The resonator size and shape can be modified to accommodate application specifications, such as room size and patient body geometry.

The key feature that distinguishes FREE-D from prior inductive schemes is the use of high-quality factor (Q factor) resonators combined with an automatic tuning scheme that keeps the system operating at maximum efficiency. The FREE-D system is able to adapt to variations in Tx–Rx separation distances, Tx–Rx orientations, and power requirements of the load. By actively controlling the frequency of the transmitted radio-frequency (RF) signal, the FREE-D system can achieve high power transfer efficiency—upwards of 90%—for nearly any angular orientation over a range of separation distances [4], [20], [21]. Table 1 summarizes the advantages of the FREE-D system over the previous TETS systems.

E. Grand Vision of the FREE-D System

The grand vision for implementing the FREE-D system with a VAD will consist of installing multiple Tx resonators throughout the household that are hidden inside walls, floors, couches, tables, and beds. There will be two Rx resonators: one will be installed in an exterior vest that will be worn by the patient, and another smaller resonator will be implanted in the human body. The larger size of the Rx vest resonator will increase the working range of the wireless power transfer. The implanted Rx resonator will be situated at a fixed distance away from the Rx vest resonator to ensure seamless energy transfer to the VAD. Therefore, the patient will be free to maneuver throughout their home while receiving wireless power from the nearest Tx resonator. Alternatively, if the patient needs to leave the home, a portable battery can temporarily provide power to the external Rx vest resonator, which will wirelessly provide power to the implanted Rx resonator and the VAD.

Table 1 Comparison of Proposed FREE-D System Versus Existing TETS System

	FREE-D	TETS
> 90% efficiency separation distance (cm)	71.0	3.0
> 50% efficiency separation distance (cm)	120	6.4
< 10% efficiency separation distance (cm)	160	10.0
> 90% efficiency angular misalignment (°)	60°	5°
> 50% efficiency angular misalignment (°)	83°	10°
< 10% efficiency angular misalignment (°)	88°	12°
Patient contact needed (yes/no)	No	Yes
Tethered operation (yes/no)	No	Yes
Energy transfer range	Meters*	10cm

* Energy transfer range depends on the size of the resonator. The FREE-D measurements in Table 1 correspond to the basic FREE-D resonator configuration in Fig. 2 with a drive resonator diameter of 31cm and a Tx and Rx resonator diameter of 59cm. The TETS data corresponds to the inductively coupled coils from [19] with a coil diameter of 85mm.

III. OVERVIEW OF THE FREE-D SYSTEM

Unlike some of the existing inductively coupled wireless power technologies currently available for consumer electronics, the FREE-D system requires dynamic power management control to operate at its full potential for improved efficiency over larger distances. The following sections outline the FREE-D wireless power circuit model as well as the additional power management circuitry. An extended analysis of the basic circuit model for magnetically coupled resonators is shown in [4].

A. Wireless Power Circuit Model

Fig. 2 shows a diagram of the basic FREE-D wireless power system. The two-element transmitter consists of a single-turn drive resonator and multiturn resonator that wirelessly transmits power to a two-element receiver. These two resonant systems efficiently exchange energy by sharing nonradiative magnetic fields that oscillate at a

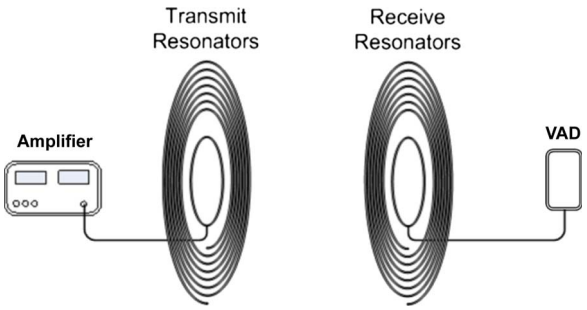

Fig. 2. *Sketch of the basic FREE-D magnetically coupled resonant wireless power system consisting of an RF amplifier capable of controlling the magnitude and frequency of the transmitted signal. A two-element transmitter wirelessly powers the two receive resonators and the load device (VAD).*

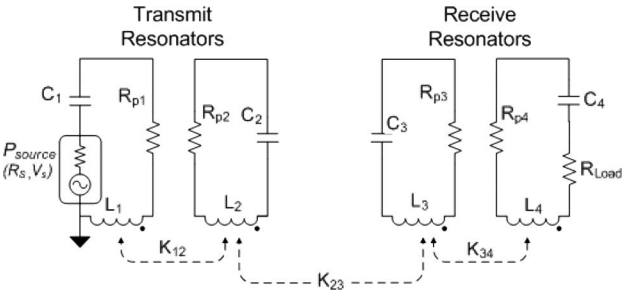

Fig. 3. *Equivalent circuit model of the basic FREE-D wireless power system. Each of the four resonators are linked by the coupling coefficients k_{12}, k_{23}, and k_{34}.*

specific resonant frequency. The most significant interaction occurs between the multiturn resonators, which are high-Q inductor–capacitor–resistor (*LCR*) tank resonators. These resonators share a mutual inductance M_{ij} that is a function of resonator geometry and separation distance between the resonators. So long as the Rx resonator is within range of the magnetic field generated by the Tx resonator, power will be transferred wirelessly between the two.

Fig. 3 shows the equivalent circuit schematic for this system in terms of the lumped circuit elements *L*, *R*, and *C*. The Tx drive loop and multiturn resonator are modeled as inductors L_1 and L_2, and the Rx multiturn resonator and drive loop are modeled as inductors L_3 and L_4, respectively. Capacitors C_1–C_4 are selected such that each magnetically coupled resonator will operate at the same resonant frequency according to

$$f_{\text{res}} = \frac{1}{2\pi\sqrt{L_i C_i}}. \tag{1}$$

The resistors R_{p1}–R_{p4} represent the parasitic resistances of each resonator, and are typically less than 1 Ω. Each resonant circuit is linked by the coupling coefficients k_{12}, k_{23}, k_{34}. These coupling coefficients are typically an order of magnitude greater than the cross coupling terms (k_{13}, k_{14}, k_{24}). The relationship between the coupling coefficient and the mutual inductance between each resonator is given in

$$k_{ij} = \frac{M_{ij}}{\sqrt{L_i L_j}}. \tag{2}$$

The transfer function in (3), shown at the bottom of the page, for the circuit model in Fig. 3 is derived using Kirchhoff's voltage law and flux linkages [4]. The transfer function neglects the cross coupling terms and is a function of frequency, inductance, capacitance, resistance, and coupling coefficients.

Fig. 4 shows the typical v-shaped efficiency plateau for the FREE-D system's magnetically coupled resonators. The coupling coefficient (k_{23}) between the Tx and Rx resonators is inversely proportional to the distance between them. As the separation distance increases, the amount of coupling between the resonators decreases, and the frequency splitting converges until the two resonant peaks converge at f_{res}.

In the overcoupled regime, the resonators share substantial magnetic flux and the system is capable of achieving maximum efficiency. At any distance in the overcoupled regime, there are two different resonant frequencies caused by the in-phase and out-of-phase modes of the overlapping magnetic fields. For any separation distance in this region, maximum efficiency can be maintained by operating at the lower frequency peak,

$$\frac{V_L}{V_s} = \frac{j\omega^3 k_{12}k_{23}k_{34}L_2L_3\sqrt{L_1L_4}R_{\text{load}}}{\left(k_{12}^2k_{34}^2L_1L_2L_3L_4\omega^4 + Z_1Z_2Z_3Z_4 + \omega^2\left(k_{12}^2L_1L_2Z_3Z_4 + k_{23}^2L_2L_3Z_1Z_4 + k_{34}^2L_3L_4Z_1Z_2\right)\right)} \tag{3}$$

$$Z_1 = R_{p1} + R_s + j\omega L_1 + \frac{1}{j\omega C_1}, \qquad Z_2 = R_{p2} + j\omega L_2 + \frac{1}{j\omega C_2}$$

$$Z_3 = R_{p3} + j\omega L_3 + \frac{1}{j\omega C_3}, \qquad Z_4 = R_{p4} + R_{\text{load}} + j\omega L_1 + \frac{1}{j\omega C_4}$$

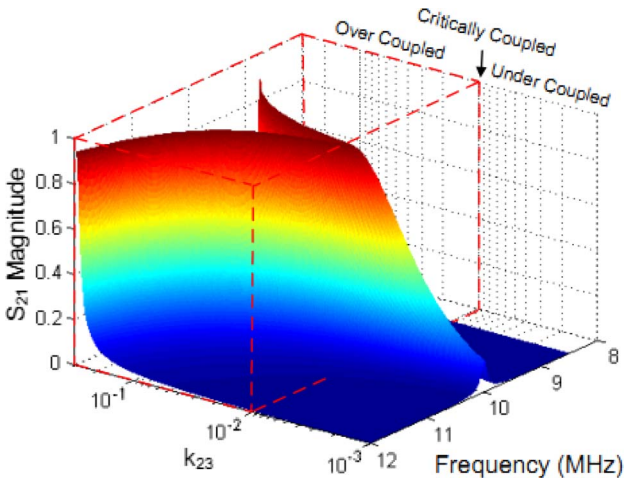

Fig. 4. *Efficiency curve for the FREE-D wireless power system resonators as a function of the coupling coefficient between the Tx and Rx multiturn resonators and frequency [4] © 2011 IEEE.*

which corresponds to the in-phase mode of the resonant system.

In the undercoupled regime, the shared flux falls below a threshold such that maximum efficiency cannot be achieved. Critical coupling is the point of transition between these two regimes, and corresponds to the greatest range at which maximum efficiency can be achieved. Similar to inductive coupling, the undercoupled regime is still capable of wireless power transfer, but the maximum achievable efficiency is limited and falls rapidly with distance.

B. Power Management Circuit Model

Power management control systems are required at both the Tx and Rx sides of the FREE-D system. The full block diagram for the FREE-D system is shown in Fig. 5.

In order to generate the alternating current (ac) waveform oscillating at a specific and controllable frequency, a directional coupler, and microcontroller unit (MCU) have been implemented with the power amplifier at the Tx side. The power amplifier delivers an RF signal through the direction coupler to the Tx resonator. The directional coupler measures the magnitude of the forward and reflected waves, which can be used to approximate the transmission power gain S_{21} of the resonators. The MCU is able to minimize the reflected power by adjusting the amplitude and frequency of the signal delivered to the Tx resonator so that maximum power transfer will occur between the Tx and Rx resonators.

At the Rx side, an RF-dc bridge rectifier is implemented to convert the oscillating RF signal to a direct current (dc) voltage. Next, a dc–dc voltage regulator steps down this rectified voltage to a constant 13.1 V_{dc}, which is required for the system controller and all VADs tested with the FREE-D system. The regulated dc voltage is delivered to the system controller, which powers the motor controller for the heart pump and monitors VAD conditions such as flow rate, pump speed, and pump power. Finally, a diode switch activates or deactivates a backup battery that can provide power to the system controller intermittently in case the FREE-D system temporarily fails. This battery will be rechargeable so that it can be charged by the FREE-D system without requiring direct access to the implanted battery itself, which requires rehospitalization.

IV. TECHNIQUES TO IMPROVE WIRELESS POWER EFFICIENCY OVER DISTANCE

There are regulatory and practical requirements that present technical challenges in integrating the FREE-D system into the homes for VAD patients. The two most significant difficulties are increasing the range at which highly efficient wireless power transfer can occur, and operating within the allowable bandwidth of the ISM bands defined by the Federal Communications Commission (FCC). Two techniques are outlined in the following sections to address these challenges including the addition of relay resonators to increase the working range of wireless power transfer, and a dynamic impedance matching network to

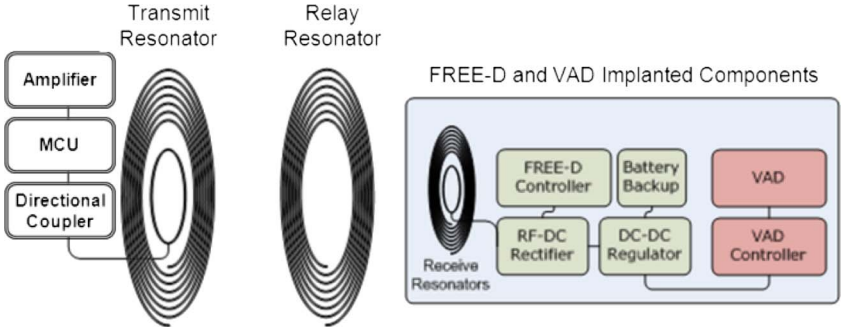

Fig. 5. *Block diagram of the complete FREE-D system showing relay resonator and implanted components.*

enable single-frequency operation in the overcoupled regime.

A. Relay Resonators

Implementing the grand vision for the application of the FREE-D system with a VAD will require several Tx resonators installed throughout the patient's home. Every Tx resonator will require its own power supply and power management system to ensure that the VAD constantly receives sufficient power as the distance between the Tx and Rx resonators increases. However, for central locations in the household away from walls and accessible electrical outlets, it will be difficult to provide the necessary equipment for each Tx resonator.

One way to avoid these potential dead zones in the center of a room would be to increase the range of the FREE-D system by increasing the size of the Tx and Rx resonators. However, for use with a VAD, the size of the Rx resonator is limited because it will be implanted in the body. Therefore, another technique using a relay resonator as in Fig. 5 can be implemented to accommodate greater separation distances between Tx and Rx resonators.

When considering the grand vision, this relay resonator configuration will allow several Tx resonators and the necessary power management circuitry to be installed in locations that have concealed access to electrical outlets (walls and floors), while freestanding relay resonators can be installed in centralized furniture (chairs, tables, and desks). These relay resonators will be able to link the wireless power transferred from the Tx resonators to the Rx vest resonator worn by the patient.

Adding a relay resonator to the basic resonator model from Fig. 2 will introduce a third resonant mode to the system in the overcoupled regime. The third mode will be centered at the resonant frequency of the system. Adding more relay resonators will continue to increase the working range of the wireless power transfer; however, the maximum achievable efficiency will decrease and the number of modes will continue to increase as more relay resonators are introduced to the system. Nonetheless, the same power management and frequency tuning algorithms will be capable of accommodating multiple-mode resonant systems.

B. Dynamic Frequency Tuning Versus Single-Frequency Operation

Unlike far-field antennas in which the input impedance of the antenna is constant, near-field antennas like the resonators in the FREE-D system have strong electromagnetic field interaction, thus the input impedance of the resonators is constantly changing as a function of the coupling or mutual inductance between the Tx and Rx resonators. As the distance between the Tx and Rx resonators increases, the coupling coefficient between the multiturn resonators decreases because the mutual inductance decreases from (2). The rectifier at the Rx side also has a complex input impedance that is changing as a function of the input power and load conditions. As a result, the impedance looking into the Tx resonator is constantly changing, making it difficult to design an impedance matching network.

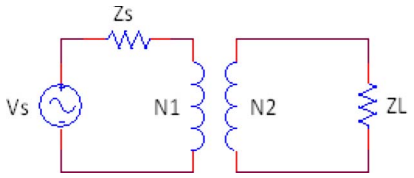

Fig. 6. *Basic air-core transformer model with source impedance Z_s and load impedance Z_L.*

The ideal solution would be to use active frequency tuning to track the maximum power transfer peaks. However, given the narrow bandwidth requirements for the ISM bands, frequency tuning will not be possible from a regulatory standpoint.

Another solution using a dynamic impedance matching network at the Tx side can be implemented to ensure that maximum power is transferred to the load at a single frequency within the ISM band. To demonstrate how this impedance matching system will work, recall the basic transformer model in Fig. 6 in which maximum power transfer is achieved when the source and load impedance are matched according to (4), where N_1 and N_2 are the number of turns of the primary and secondary coils, respectively

$$Z_s = \left(\frac{N_1}{N_2}\right)^2 Z_L \tag{4}$$

The FREE-D Tx and Rx resonators can be thought of as an air-core transformer with complex source and load impedances. Therefore, a π-match filter can be implemented as in Fig. 7 to perform conjugate impedance matching. Similar to changing the turns ratio in the basic transformer model to perform real impedance matching, the π-match filter can perform conjugate impedance matching when proper values of L, C_s, and C_L are chosen.

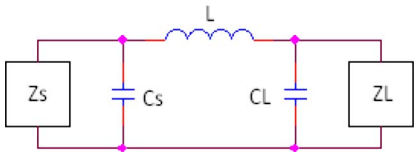

Fig. 7. *Basic π-match two-port network to match source impedance Z_s to load impedance Z_L.*

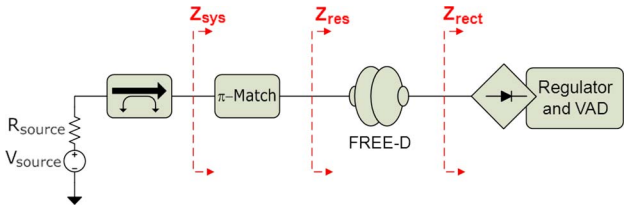

Fig. 8. *Block diagram of the π-match filter implemented with the FREE-D system for use with a VAD.*

Since the source and load impedances vary as the distance between the Tx and Rx resonators changes, by dynamically selecting the capacitor values C_s and C_L in the π-match filter, the source and load impedances will always be matched.

Rather than using frequency tracking, this impedance matching technique will deliver maximum power to the load while operating at a single frequency. Fig. 8 shows how the π-match filter can be implemented with the FREE-D system.

A Matlab model has been developed that uses *S*-parameter data collected from a vector network analyzer (VNA) for any set of magnetically coupled resonators. Fig. 9 shows a basic block diagram of how the Matlab model is implemented.

The input impedance of the resonators Z_{res} can be calculated from the S-parameter data using S_{11}. By defining the resonant frequency and the π-match inductor value L, the Matlab model calculates the values of C_s and C_L that match the source impedance R_{source} and the load impedance Z_{res}. The parasitic resistances of the capacitors R_{PS} and R_{PL} and the inductor in the π-match filter can be defined in the Matlab model for improved accuracy.

As a proof of concept, this dynamic impedance matching model has been tested with the set of coils shown in Fig. 10.

The PCB coils were tuned to resonate at 13.56 MHz. The same sized drive loop and multiturn coil were used for both the Tx and the Rx. The loop-coil distance was fixed at 1 cm and the Tx coil to Rx coil distance was

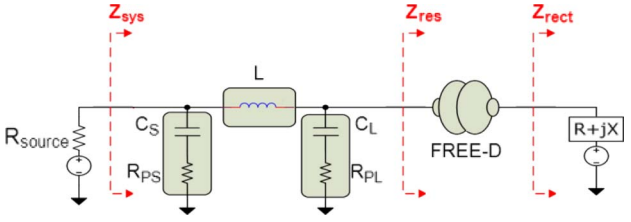

Fig. 9. *Block diagram of the π-match filter Matlab model showing the π-match filter, the FREE-D resonators, and the complex rectifier impedance indicated by $R + jX$.*

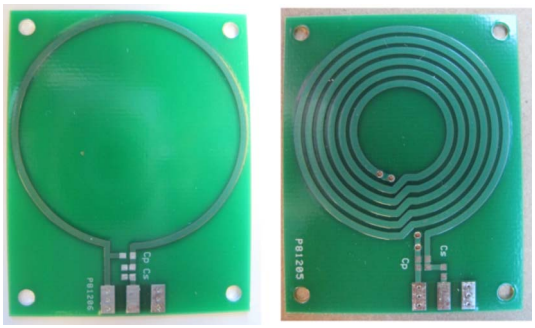

Fig. 10. *PCB coils used for Matlab model proof of concept. The drive loop (left) is 4.3 cm in diameter, and the multiturn coil (right) is 4.0 cm in diameter.*

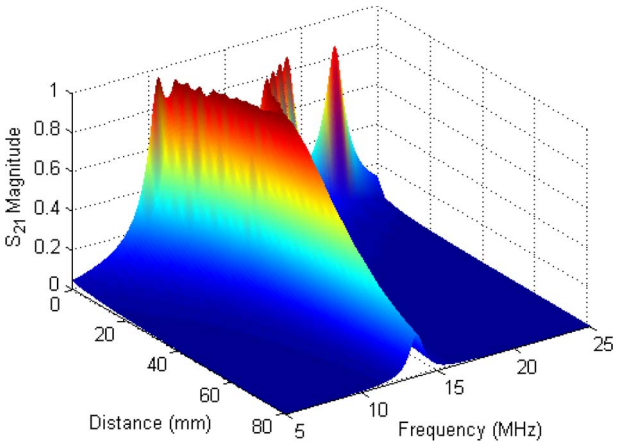

Fig. 11. *Efficiency curve for PCB coils shown in Fig. 10 as a function of separation distance between Tx and Rx coils and frequency.*

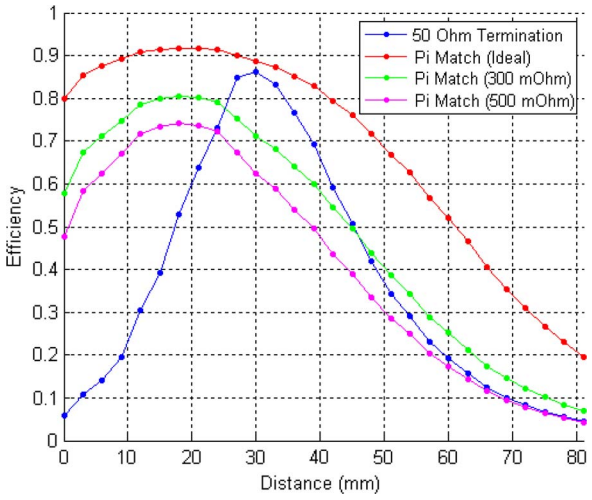

Fig. 12. *Efficiency comparisons of the 50-Ω termination impedance data and the π-match simulation model at a single frequency.*

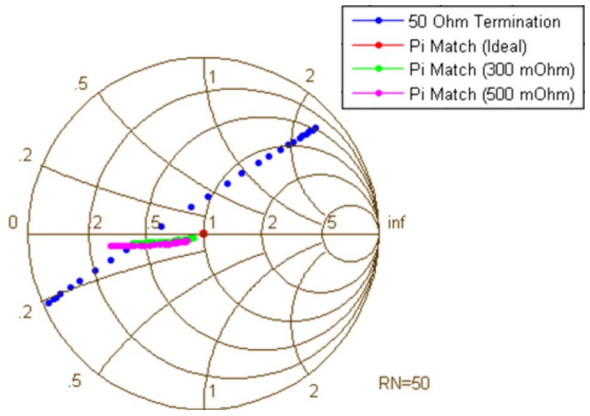

Fig. 13. *Smith chart comparisons of the 50-Ω termination impedance data and the π-match simulation model at a single frequency.*

incremented by 5 mm until a maximum distance of 80 mm was reached. S-parameter data were collected by the VNA at each distance increment with 50-Ω termination impedances at both the source and the load. The v-shaped efficiency curve for this raw coil data can be seen in Fig. 11.

These *S*-parameter data were then imported into the π-match Matlab model. For a resonant frequency of 13.56 MHz, a source and load impedance of 50 Ω, and a π-match inductor value of 200 nH, Fig. 12 shows a comparison of the single-frequency wireless power transfer efficiencies for the 50-Ω termination impedance data, the ideal π-match filter simulation, and the π-match filter simulation including parasitic resistances.

Without the π-match filter, the efficiency (blue curve in Fig. 12) is minimal in the overcoupled regime where frequency splitting occurs in Fig. 11. For the ideal π-match filter simulation (red curve in Fig. 12), the impedance Z_{res} is perfectly matched to the 50-Ω source impedance, resulting in the highest possible wireless power transfer efficiency. As the parasitic resistances increase (green and magenta curves in Fig. 12), the efficiency decreases due to losses across the resistors. However, this parasitic model will more accurately represent the behavior of the experimental system.

Fig. 13 shows the Smith chart for each of the simulation models from Fig. 12. The 50-Ω termination impedance data (blue data in Fig. 13) shows that the impedance Z_{res} changes as the distance between the Tx and Rx coils changes. The ideal π-match filter simulation (red data in Fig. 13) shows a perfect match to 50 Ω for all distances, while the π-match filter simulation with parasitic resistances (green and magenta data in Fig. 13) shows a strong reactive impedance match, but a mismatch in resistance.

A switching circuit can be implemented to switch on or off source and load capacitors in the π-match filter. The dynamic impedance matching model quickly determines the necessary π-match component values to enable single-frequency operation for any magnetically coupled resonators.

Fig. 14. *An axial pump (HeartMate II, Thoratec, Pleasanton, CA).*

Fig. 15. *A centrifugal pump (VentrAssist LVAD).*

V. IMPLEMENTATION AND EXPERIMENTAL RESULTS

The various resonator configurations discussed in previous sections have been experimentally tested using the

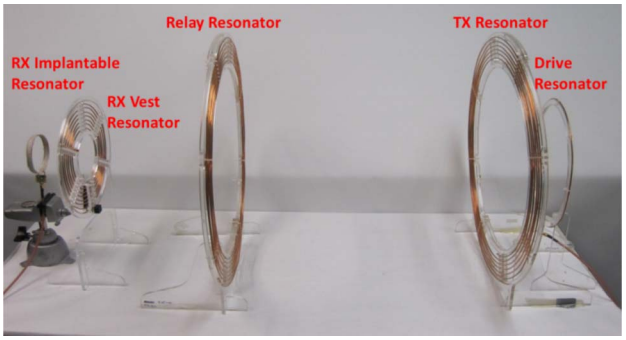

Fig. 16. *FREE-D resonator configuration for both the axial and centrifugal VAD pump experiments.*

Table 2 Resonator Sizes for FREE-D Experimental Configuration

Resonator Description	Diameter (cm)
Drive Resonator	31
TX Resonator	59
Relay Resonator	59
RX Vest Resonator	28
RX Implantable Resonator	9.5

FREE-D wireless power system with both the commercially available axial pump and VentrAssist VADs shown in Figs. 14 and 15, respectively.

Two separate experiments have been conducted to monitor various components of the FREE-D system including the consistency of power delivery to the VAD and the efficiency of the FREE-D resonators, rectifier, and regulator. The resonator configuration for both experiments is shown in Fig. 16, and the resonator sizes are shown in Table 2. Relay resonators are included to enable wireless power transfer over meter distances.

A. Axial VAD Experiment

The resonator configuration for the first experiment using the FREE-D system to wirelessly power the axial VAD can be seen in Fig. 17.

An 8-h continuous time experiment was conducted with the FREE-D resonators separated by a 1-m distance. Power of 8.1 W was required to power the axial VAD operating at a typical pump speed of 2400 r/min. Voltage and current measurements were taken every 15 s both before and after the FREE-D resonators, the RF-dc rectifier and the dc–dc regulator to calculate the efficiency of each component. Fig. 18 shows the constant power delivery to the VAD over the entire 8-h time period, verifying the successful implementation of the FREE-D system. Fig. 19 shows the coil efficiency, the RF-dc rectifier efficiency, and the dc–dc regulator efficiency over the 8-h time period. The FREE-D system efficiency is approximately 56% for this experiment. This efficiency can be improved in future experiments by optimizing the resonator efficiency and implementing the dynamic impedance matching system.

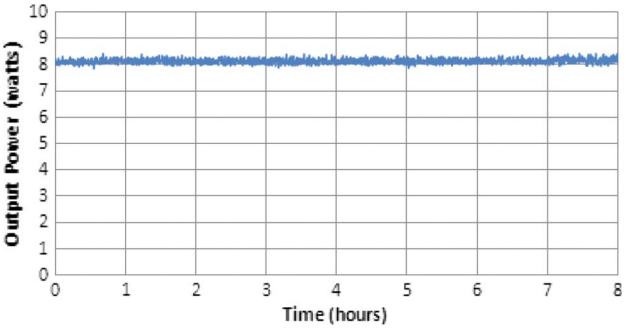

Fig. 18. *Plot showing a constant output power of 8.1 W delivered to the axial VAD for the entire 8-h time period for a pump speed of 2400 r/min.*

B. VentrAssist VAD Experiment

The goal of this experiment is to demonstrate a successful implementation of the FREE-D system with the Ventracor VentrAssist centrifugal VAD for an extended two-week time period over the entire range of pump speeds. The VentrAssist computer software allows for quick changes to the pump conditions. Pump speeds were increased periodically by 200 r/min from the minimum speed (1800 r/min) to the maximum speed (3000 r/min) over the course of two weeks. The VentrAssist software logs VAD pump power, speed, and flow rate data every second. The resonator configuration for this experiment with the centrifugal VAD is shown in Fig. 20. The backup battery that can be used for temporary faults in wireless power transfer is also shown in Fig. 20; however, it

Fig. 17. *Configuration for the axial VAD experiment showing the VAD being wirelessly powered via the FREE-D system, which is connected to the RF-dc rectifier and dc–dc regulator circuit and the HeartMate II System Controller.*

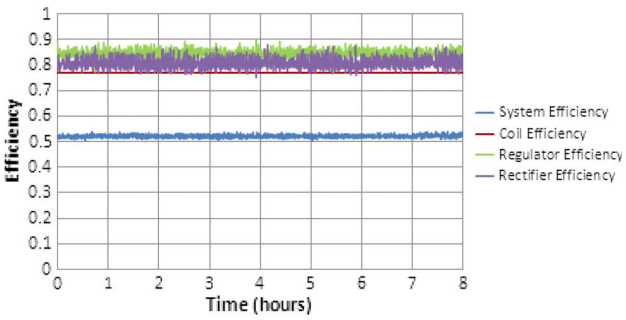

Fig. 19. *Efficiency of the FREE-D components over the 8-h time period for a pump speed of 2400 r/min with the axial VAD.*

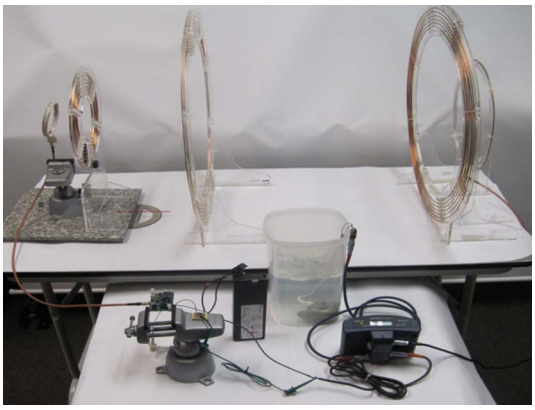

Fig. 20. *Configuration for the VentrAssist VAD experiment showing the VAD being wirelessly powered via the FREE-D system, which is connected to the RF-dc rectifier and dc–dc regulator circuit and the VentrAssist System Controller. An unplugged backup battery is also shown.*

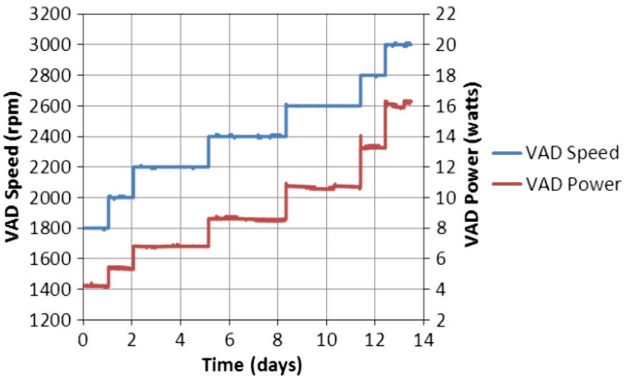

Fig. 21. *Plot showing the steady output power delivered to the centrifugal VAD for the entire two-week time period over a full range of pump speeds.*

remained unplugged for the entire duration of this experiment.

As the pump speed increases over the course of the two-weeks, the power demanded by the pump increases. Fig. 21 shows the VAD pump speed and corresponding pump power over the entire two-week duration. This plot verifies that the FREE-D system can wirelessly power the centrigual VAD for an extended period of time without a single fault.

The efficiencies of the FREE-D components are shown in Fig. 22. For this experiment, the resonator efficiency

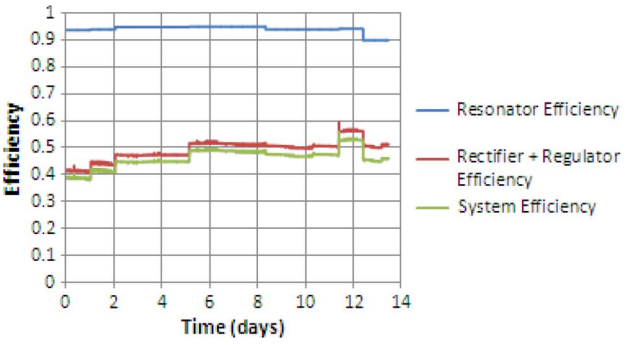

Fig. 22. *Efficiency of the FREE-D components over the two-week time period for a full range of pump speeds with the centrifugal VAD. The rectifier efficiency refers to the efficiency of both the RF-dc rectifier and the dc–dc regulator.*

was maximized by slightly changing the position of the relay resonator for the static resonator configuration in Fig. 20. Although the resonator efficiency is upwards of 90% for every pump speed, the rectifier efficiency—which also accounts for the regulator efficiency in this experiment—significantly reduces the system efficiency. This inefficiency is primarily due to an impedance mismatch between the rectifier and the impedance of the VAD, and can be improved in future experiments by implementing the impedance matching system.

VI. CONCLUSION AND FUTURE WORK

FREE-D technology could be applied in other medical applications that require unobtrusive recharging of implanted batteries, such as pacemakers, implanted defibrillators, cochlear implants, or retinal implants. Outside medicine, some ideal consumer electronic applications include mobile phone charging, electric car charging, and kitchen appliance operation.

Future work for the FREE-D system to power VADs includes a full characterization of relay resonators presented here, and a study on the effects that conductive materials (human body tissues, batteries, and implanted circuitry) have on power transfer efficiency. Also, the dynamic impedance matching model will be integrated with the FREE-D resonators to improve the system efficiency and enable single-frequency operation. To progress towards clinical deployment, animal trials with our next generation FREE-D system are planned. ■

REFERENCES

[1] R. J. Gordon, B. Quagliarello, and F. D. Lowy, "Ventricular assist device-related infections," *Lancet Infect Dis.*, vol. 6, no. 7, pp. 426–437, Jul. 2006.

[2] *HeartMate II LVAS Operating Manual*, Thoratec Corporation, Mar. 2010.

[3] *VentrAssist LVAS Clinical Instructions for Use*, Ventracor, 2010.

[4] A. Sample, D. Meyer, and J. R. Smith, "Analysis, experimental results, and range adaptation of magnetically coupled resonators wireless power transfer," *IEEE Trans. Ind. Electron.*, vol. 58, no. 2, pp. 544–554, Feb. 2011.

[5] M. C. Deng, L. B. Edwards, M. I. Hertz, A. W. Rowe, and R. L. Kormos, "Mechanical circulatory support device database of the international society for heart and lung transplantation: First annual report—2003," *J. Heart Lung Transplant*, vol. 22, no. 6, pp. 653–662, Jun. 2003.

[6] L. W. Miller, F. D. Pagani, S. D. Russell, R. John, A. J. Boyle, K. D. Aaronson, J. V. Conte, Y. Naka, D. Mancini, R. M. Delgado, T. E. MacGillivray, D. J. Farrar, and O. H. Frazier, "HeartMate II

clinical investigators. Use of a continuous-flow device in patients awaiting heart transplantation," *New England J. Med.*, vol. 357, no. 9, pp. 885–896, Aug. 30, 2007.

[7] F. D. Pagani, L. W. Miller, S. D. Russell, K. D. Aaronson, R. John, A. J. Boyle, J. V. Conte, R. C. Bogaev, T. E. MacGillivray, Y. Naka, D. Mancini, H. T. Massey, L. Chen, C. T. Klodell, J. M. Aranda, N. Moazami, G. A. Ewald, D. J. Farrar, and O. H. Frazier, "HeartMate II investigators. Extended mechanical circulatory support with a continuous-flow rotary left ventricular assist device," *J. Amer. Coll. Cardiol.*, vol. 54, no. 4, pp. 312–321, Jul. 21, 2009.

[8] S. I. Martin, L. Wellington, K. B. Stevenson, J. E. Mangino, C. B. Sai-Sudhakar, M. S. Firstenberg, D. Blais, and B. C. Sun, "Effect of body mass index and device type on infection in left ventricular assist device support beyond 30 days," *Interact. Cardiovasc. Thorac. Surg.*, vol. 11, no. 1, pp. 20–23, Jul. 2010.

[9] W. L. Holman, S. V. Pamboukian, D. C. McGiffin, J. A. Tallaj, M. Cadeiras, and J. K. Kirklin, "Device related infections: Are we making progress?" *J. Card. Surg.*, vol. 25, no. 4, pp. 478–483, Jul. 2010.

[10] A. L. Raymond, A. G. Kfoury, C. J. Bishop, E. S. Davis, K. M. Goebel, S. Stoker, C. H. Selzman, S. E. Clayson, H. Smith, C. G. Cowley, R. Alharethi, D. Budge, and B. B. Reid, "Obesity and left ventricular assist device driveline exit site infection," *ASAIO J.*, vol. 56, no. 1, pp. 57–60, Jan./Feb. 2010.

[11] A. Zierer, S. J. Melby, R. K. Voeller, T. J. Guthrie, G. A. Ewald, K. Shelton, M. K. Pasque, M. R. Moon, R. J. Damiano, Jr., and N. Moazami, "Late-onset driveline infections: The Achilles' heel of prolonged left ventricular assist device support," *Ann. Thorac. Surg.*, vol. 84, no. 2, pp. 515–520, Aug. 2007.

[12] J. G. Allen, E. S. Weiss, J. M. Schaffer, N. D. Patel, S. L. Ullrich, S. D. Russell, A. S. Shah, and J. V. Conte, "Quality of life and functional status in patients surviving 12 months after left ventricular assist device implantation," *J. Heart Lung Transplant*, vol. 29, no. 3, pp. 278–285, Mar. 2010.

[13] W. Wilson, K. A. Taubert, M. Gewitz, P. B. Lockhart, and L. M. Baddour, "Prevention of infective endocarditis," *J. Amer. Dent. Assoc.*, vol. 139, no. Suppl:3S–24S, Jan 2008.

[14] D. H. Monkowski, P. Axelrod, T. Fekete, T. Hollander, S. Furukawa, and R. Samuel, "Infections associated with ventricular assist devices: Epidemiology and effect on prognosis after transplantation," *Transpl. Infect. Dis.*, vol. 9, no. 2, pp. 114–120, Jun. 2007.

[15] V. K. Topkara, S. Kondareddy, F. Malik, I. W. Wang, D. L. Mann, G. A. Ewald, and N. Moazami, "Infectious complications in patients with left ventricular assist device: Etiology and outcomes in the continuous-flow era," *Ann. Thorac. Surg.*, vol. 90, no. 4, pp. 1270–1277, Oct. 2010.

[16] A. Mizannojehdehi, M. Shams, and T. Mussivand, "Design and analysis of a class-e frequency-controlled transcutaneous energy transfer system," in *Proc. IEEE Electron. Circuits Syst. Conf.*, Dec. 2006, pp. 21–24.

[17] S. Haj-Yahia, E. J. Birks, P. Rogers, C. Bowles, M. Hipkins, R. George, M. Amrani, M. Petrou, J. Pepper, G. Dreyfus, and A. Khaghani, "Midterm experience with the Jarvik 2000 axial flow left ventricular assist device," *J. Thorac. Cardiovasc. Surg.*, vol. 134, no. 1, pp. 199–203, Jul. 2007.

[18] A. El-Banayosy, L. Arusoglu, L. Kizner, M. Morshuis, G. Tenderich, W. E. Pae, Jr., and R. Körfer, "Preliminary experience with the LionHeart left ventricular assist device in patients with end-stage heart failure," *Ann. Thorac. Surg.*, vol. 75, no. 5, pp. 1469–1475, May 2003.

[19] T. Ozeki, T. Chinzei, Y. Abe, I. Saito, T. Isoyama, S. Mochizuki, M. Ishimaru, K. Takiura, A. Baba, T. Toyama, and K. Imachi, "Functions for detecting malposition of transcutaneous energy transmission coils," *ASAIO J.*, vol. 49, pp. 469–474, Jul. 2003.

[20] J. Smith, A. Sample, B. Waters, Y. Toyoda, R. Kormos, and P. Bonde, "Innovative free-range resonant electrical energy delivery system (FREE-D system) for a ventricular assist device (VAD) using wireless power," in *Proc. ASAIO 31st Annu. Conf.*, Washington, DC, Jun. 10–12, 2011, p. 102.

[21] P. Bonde, A. Sample, B. Waters, E. Cooper, Y. Toyoda, R. Kormos, and J. Smith, "Wireless power for ventricular assist devices: Innovation with the free-range resonant electrical energy delivery system (FREE-D) for mechanical circulatory assist," in *Proc. AATS 91st Annu. Sci. Meeting*, Philadelphia, PA, May 7–11, 2011, pp. 1–4.

ABOUT THE AUTHORS

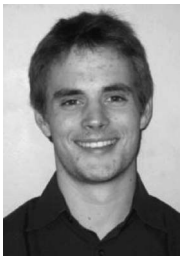

Benjamin H. Waters (Student Member, IEEE) received the B.A. degree in physics from Occidental College, Los Angeles, CA, in 2010 and the B.S. degree in electrical engineering from Columbia University, New York, NY, in 2010, as part of the 3-2 Combined Plan. He is currently working towards the Ph.D. degree in electrical engineering at the University of Washington, Seattle.

As an undergraduate, he worked in the Columbia Integrated Systems Laboratory (CISL) at Columbia University where he completed research on wireless power transfer. He has several internship experiences with Network Appliance, Arup, and most recently with Intel Labs Seattle in 2010 where he continued his research in wireless power transfer. His research interests lie mostly in the field of wireless power, including near-field antenna design, adaptive maximum power point tracking systems, and applications for these systems including biomedical, military, and consumer electronics.

Mr. Waters is a member of Tau Beta Pi and Pi Mu Epsilon.

Alanson P. Sample (Student Member, IEEE) received the B.S. and M.S. degrees in electrical engineering from the University of Washington (UW), Seattle, in 2005 and 2008, respectively, where he is currently working towards the Ph.D. degree in electrical engineering.

He is currently a Postdoctoral Research Associate in the Computer Science and Engineering Department at the UW. Throughout his graduate studies, he worked at Intel Labs Seattle as both a full time employee and as an intern. During his time at Intel, he published several articles on the use of magnetically coupled resonators for wireless power delivery, as well as papers on RFID and ambient RF energy harvesting. He was one of the key contributors to the Wireless Identification and Sensing Platform, which was open-sourced in 2009 as part of Intel s WISP Challenge. His research interests lie broadly in the area of wireless power including: antenna theory and design, energy harvesting from ambient and deliberate sources, novel sensing and computing elements, and the application of these systems.

Pramod Bonde (Member, IEEE) received the M.D. and M.S. degrees from the University of Bombay, Bombay, India, in 1991 and 1996, respectively, and the FRCS and FRCS (CTh) degrees from the University of Glasgow, Glasgow, U.K., in 1999 and 2007, respectively.

He is a heart surgeon specializing in the treatment of end stage heart failure by means of heart pumps. He has extensive clinical experience in treating heart failure with all available artificial heart pump technologies. His clinical focus is on expanding the indications so as to benefit a much wider patient population who are currently denied access to such life saving technology due to age or co-morbidities. His research work is focused towards medical devices and development of mechanical circulatory support systems. He is especially interested in making the artificial heart systems more patient friendly and to reduce the adverse events associated with such technology. His work includes development of a tether free heart assist system that can be inserted using key hole surgery so as to allow quick recovery and unparalleled freedom to his patients. He is the Director of Mechanical Circulatory Support and an Assistant professor of Surgery at Yale School of Medicine.

Joshua R. Smith (Member, IEEE) received the B.A. degree in computer science and philosophy from Williams College, Williamstown, MA, in 1991, the M.A. degree in physics from Cambridge University, Cambridge, U.K., in 1997, and the S.M. and Ph.D. degrees from the MIT Media Lab, Cambridge, in 1995 and 1999, respectively.

He is an Associate Professor of Electrical Engineering and of Computer Science and Engineering at the University of Washington, Seattle, where he leads the Sensor Systems research group. From 2004 to 2010, he was Principal Engineer at Intel Labs Seattle. He is interested in all aspects of sensor systems, including creating novel sensor systems, powering them wirelessly, and using them in applications such as robotics, ubiquitous computing, and human–computer interaction. At Intel, he founded and led the Wireless Resonant Energy Link (WREL) project, as well as the Wireless Identification and Sensing Platform (WISP) project, and the Personal Robotics project. Previously, he coinvented an electric field sensing system for suppressing unsafe airbag firing that is included in every Honda car.